Signal Processing 128 (2016) 350–359

Contents lists available at ScienceDirect

Signal Processing

journal homepage: www.elsevier.com/locate/sigpro

Two-stage DOA estimation of independent and coherent signals in spatially coloured noise

Yuexian Wang*, Matthew Trinkle, Brian W.-H. Ng

University of Adelaide Radar Research Centre, School of Electrical and Electronic Engineering, The University of Adelaide, South Australia, SA 5005, Australia

ARTICLE INFO

Article history:
Received 29 September 2015
Received in revised form
27 April 2016
Accepted 28 April 2016
Available online 6 May 2016

Keywords:
Direction of arrival (DOA)
Coherent signals
Coloured noise
Matrix reconstruction

ABSTRACT

A novel fourth order cumulant-based matrix reconstruction algorithm is presented for direction of arrival (DOA) estimation when both independent and coherent signals coexist in the presence of spatially coloured noise. The method operates in two stages. By exploiting the orthogonality between subspaces, the DOA estimates of uncorrelated sources are first obtained, then the independent components are eliminated by reconstructing the corresponding cumulant matrix. Secondly, a series of matrix reconstructions are performed, then the remaining coherent sources are resolved from the reconstructed matrix which has been rank restored. The resultant algorithm can resolve more signals than array elements with higher accuracy and better classification of signal type than previous methods. Simulation results demonstrate the validity and efficiency of the proposed method.

1. Introduction

Sensor arrays have been used in many fields such as radar, sonar, telecommunication, geophysical exploration, etc. [1]. Direction of arrival (DOA) estimation of incident signals, as an important topic in array processing, has drawn a considerable amount of attention, and many prominent eigensystem-based methods, such as MUSIC [2] and ESPRIT [3], have been proposed for dealing with this issue. However, these high-resolution methods are unable to work when uncorrelated and coherent signals coexist, which make the spatial covariance matrix deficient in rank. This situation typically results from multipath propagation in real environments.

To combat signal coherency, many rank recovery algorithms [4–6] have been proposed, where forward/backward spatial smoothing (FBSS) [5] is the most common, but results in poor utilisation of array elements since it resolves all the uncorrelated, partially coherent or fully coherent signals simultaneously.

To deal with this problem a pre-processing step that estimates and removes the uncorrelated signals prior to FBSS is typically applied [7–10]. One of the first publications which used spatial differencing to remove the uncorrelated signals was that of Rajagopal et al. [7]. However, their initial algorithm could only resolve two sources in each coherent group. This work was followed up by Qi et al. [8] and Ye et al. [9]. Both approaches made better use of the degrees of freedom (DOF) of the sensor array, but the algorithm by Qi et al. was verified only by simulation without a theoretical proof, while the method by Ye et al. is not robust to certain angular separations. In [10] an alternative approach to spatial differencing is presented. The uncorrelated signals are removed by subtracting their reconstructed covariance matrix, which gives better accuracy than spatial differencing.

The methods reviewed above are based just on second order statistics (SOS) of the received data. Since high order statistics contain distinct characteristics, algorithms based on fourth order cumulants (FOC) have a significantly larger estimation capacity than SOS methods. Also they are insensitive to coloured noise which is a thorny problem for SOS approaches. Several direction-finding methods [11–13] based on FOC have been developed for non-Gaussian signals in the presence of multipath propagation. In [11,12], the virtual ESPRIT algorithm (VESPA) was extended to the case of coherent signals. By blindly estimating the generalised steering vectors the DOAs of coherent signals in each group can be determined, and VESPA can thus estimate significantly more coherent signals than the number of sensor. As dealing with independent and coherent signals separately has a clear advantage in DOF as well, it is promising to combine the two-stage processing strategy with fourth order statistics. However, this work has rarely been investigated, and we have only found one contribution in this area which is FOC-based spatial difference smoothing, referred to as FSDS [13]. The method can handle more signals than the number of sensor, similarly to VESPA, but no direct comparison has been carried out so far.

* Corresponding author.
E-mail addresses: jwang@eleceng.adelaide.edu.au (Y. Wang), mtrinkle@eleceng.adelaide.edu.au (M. Trinkle), brian.ng@adelaide.edu.au (B.-H. Ng).

http://dx.doi.org/10.1016/j.sigpro.2016.04.015
0165-1684/

In this correspondence, a new FOC-based two-stage DOA estimation method is introduced for the case when independent and coherent signals coexist in spatially coloured noise. The main differences between our method and FSDS lie in: (a) our method employs more FOC matrices to achieve the consistent estimates of the signal and noise subspaces, so the orthogonality between the two subspaces is expected to hold more stably and gives rise to a lower estimation error of independent signals, while FSDS ignores such information, which restricts the estimation accuracy; (b) the number of signals, both independent and coherent, may not be available in real applications. To identify the independent signals from the coherent ones, we provide a source enumeration method, whereas FSDS attempts to solve this issue by comparing differences between twice estimates, but scant details on how to set the threshold for the differences are provided; (c) our approach eliminates the independent components through subtraction of the reconstructed cumulant matrix of independent signals without removing any coherent signal information, whereas FSDS achieves the same goal by using spatial differencing which loses part of the coherent signal information, resulting in degraded estimation performance of coherent signals; (d) a new rank restoration technique, which makes use of all entries of the cumulant matrix of the coherent signals is developed in our algorithm, whereas the rank restoration technique adopted by FSDS follows a similar idea as standard spatial smoothing [4] and is just tailored to alleviate pseudo-DOA estimates caused by the differencing operation. Combined together, these differences mean that our method can offer better estimation performance.

The rest of the paper is organised as follows. In Section 2, the signal model when independent and coherent signals coexist is presented. In Section 3, we provide a two-stage preprocessing strategy to estimate the DOAs of the independent and coherent signals separately. In Section 4, simulation results show the validity and efficiency of our proposed method. Finally, some concluding remarks are given in Section 5.

Throughout this paper, the following notations will be used: the operators $(\cdot)^T$, $(\cdot)^*$, $(\cdot)^H$, $(\cdot)^{-1}$, $(\cdot)^+$, $E[\cdot]$, $\|\cdot\|_F$, $\lceil\cdot\rceil$, and $\lfloor\cdot\rfloor$ denote the operation of transpose, conjugate, conjugate transpose, inverse, pseudo-inverse, expectation, Frobenius norm, ceiling, and flooring of a decimal number, respectively. The imaginary number symbol j is defined by $j=\sqrt{-1}$. The symbol $\mathrm{diag}\{z_1, z_2\}$ represents a diagonal matrix with diagonal entries z_1, z_2 and $\mathrm{blkdiag}\{\mathbf{Z}_1, \mathbf{Z}_2\}$ represents a block diagonal matrix with diagonal entries $\mathbf{Z}_1$, $\mathbf{Z}_2$. The symbol $\mathrm{rank}(\mathbf{Z})$ denotes the rank of a matrix $\mathbf{Z}$. The symbol $\mathbf{Z}(a{:}\ b, c{:}\ d)$ denotes a constructed submatrix by the entries from a to b-th row and c to d-th column of $\mathbf{Z}$, and the symbol $\mathbf{Z}(a, b)$ denotes the entry in the a-th row and b-th column of $\mathbf{Z}$.

2. Problem formulation

Consider a number of N narrowband far-field signals impinging on a uniform linear array with M identical omnidirectional sensors. Assume that there are K groups of coherent signals, which come from K statistically independent far-field sources $s_k(t)$ with power σ_k^2 for $k = 1, 2, \ldots, K$, and with P_k multipath signals for each source. In the k-th coherent group, the signal coming from direction θ_{kp}, $p = 1, 2, \ldots, P_k$ corresponds to the p-th multipath propagation of the source $s_k(t)$, and the complex fading coefficient is α_{kp}. Denote the total number of coherent signals as $N_c = \sum_{k=1}^{K} P_k$, and assume the remaining $N_u = N - N_c$ sources $s_k(t)$ coming from direction θ_k with power σ_k^2, $k = N_c+1, N_c+2, \ldots, N$, are independent to each other and also to the coherent signals. The $M \times 1$ array output vector is then given by

$$\mathbf{x}(t) = \sum_{k=1}^{K}\sum_{p=1}^{P_k} \mathbf{a}(\theta_{kp})\alpha_{kp}s_k(t) + \sum_{k=N_c+1}^{N} \mathbf{a}(\theta_k)s_k(t) + \mathbf{n}(t)$$
$$= \mathbf{A}_c\boldsymbol{\Gamma}\mathbf{s}_c(t) + \mathbf{A}_u\mathbf{s}_u(t) + \mathbf{n}(t) = \bar{\mathbf{A}}\mathbf{s}(t) + \mathbf{n}(t) \tag{1}$$

where $\mathbf{a}(\theta) = \left[1, e^{j\frac{2\pi d}{\lambda}\sin\theta}, \ldots, e^{j\frac{2\pi(M-1)d}{\lambda}\sin\theta}\right]^T \in \mathbb{C}^M$ is the steering vector with λ and d being the wavelength of carrier signal and the spacing between adjacent elements, respectively, $\mathbf{A}_c = [\mathbf{A}_{c,1}, \ldots, \mathbf{A}_{c,K}]$ with $\mathbf{A}_{c,k} = \left[\mathbf{a}(\theta_{k1}), \ldots, \mathbf{a}(\theta_{kP_k})\right]$, $\boldsymbol{\Gamma} = \mathrm{blkdiag}\{\boldsymbol{\alpha}_1, \ldots, \boldsymbol{\alpha}_K\}$ with $\boldsymbol{\alpha}_k = [\alpha_{k1}, \ldots, \alpha_{kP_k}]^T$ containing attenuation information of the k-th coherent group, $\mathbf{A}_u = \left[\mathbf{a}(\theta_{N_c+1}), \mathbf{a}(\theta_{N_c+2}), \ldots, \mathbf{a}(\theta_N)\right]$, $\mathbf{s}_c(t) = [s_1(t), \ldots, s_K(t)]^T$, $\mathbf{s}_u(t) = \left[s_{N_c+1}(t), \ldots, s_N(t)\right]^T$, $\bar{\mathbf{A}} = [\mathbf{A}_c\boldsymbol{\Gamma}, \mathbf{A}_u] = \left[\bar{\mathbf{a}}_1, \ldots, \bar{\mathbf{a}}_{K+N_u}\right]$, $\mathbf{s}(t) = \left[\mathbf{s}_c^T(t), \mathbf{s}_u^T(t)\right]^T$, and $\mathbf{n}(t)$ is spatially coloured Gaussian noise with an unknown covariance matrix. Besides, we assume that the array is calibrated, and the array manifold $\bar{\mathbf{A}}$ is unambiguous, i.e., the steering vectors $\{\mathbf{a}(\theta_i)\}_{i=1}^N$ are linearly independent for any set of distinct $\{\theta_i\}_{i=1}^N$. Equivalently, the matrix $\bar{\mathbf{A}}$ is of full column rank.

Based on the definition of cumulants and recalling the property [CP1], [CP3], [CP5], and [CP6] in [14], the array FOC matrix is given by

$$\mathbf{C}_{x,i} \triangleq \mathrm{cum}\{x_i(t), x_i^*(t), \mathbf{x}(t), \mathbf{x}^H(t)\}$$
$$= E[x_i(t)x_i^*(t)\mathbf{x}(t)\mathbf{x}^H(t)] - E[x_i(t)x_i^*(t)]E[\mathbf{x}(t)\mathbf{x}^H(t)]$$
$$- E[x_i(t)\mathbf{x}(t)]E[x_i^*(t)\mathbf{x}^H(t)] - E[x_i(t)\mathbf{x}^H(t)]E[x_i^*(t)\mathbf{x}(t)]$$
$$= \sum_{k=1}^{K+N_u} |\bar{\mathbf{A}}(i, k)|^2 \bar{\mathbf{a}}_k\bar{\mathbf{a}}_k^H \mathrm{cum}\{s_k(t), s_k^*(t), s_k(t), s_k^*(t)\}$$
$$= \sum_{k=1}^{K+N_u} \gamma_k |\bar{\mathbf{A}}(i, k)|^2 \bar{\mathbf{a}}_k\bar{\mathbf{a}}_k^H = \bar{\mathbf{A}}\mathbf{C}_{s,i}\bar{\mathbf{A}}^H, \quad i = 1, 2, \ldots, M \tag{2}$$

where $\gamma_k \triangleq \mathrm{cum}\{s_k(t), s_k^*(t), s_k(t), s_k^*(t)\}$ and $\mathbf{C}_{s,i} \triangleq \mathrm{diag}\{\gamma_1|\bar{\mathbf{A}}(i, 1)|^2, \ldots, \gamma_{K+N_u}|\bar{\mathbf{A}}(i, K+N_u)|^2\}$. In order to improve the robustness of cumulant matrix estimates, we can take the average of them as the final estimate, i.e.,

$$\mathbf{C}_x = \frac{1}{M}\sum_{i=1}^{M} \mathbf{C}_{x,i} = \bar{\mathbf{A}}\mathbf{C}_s\bar{\mathbf{A}}^H \tag{3}$$

where

$$\mathbf{C}_s = \mathrm{diag}\{\bar{\gamma}_1, \ldots, \bar{\gamma}_{K+N_u}\} \tag{4}$$

with $\bar{\gamma}_k \triangleq \frac{\gamma_k}{M}\sum_{i=1}^{M}|\bar{\mathbf{A}}(i, k)|^2$.

3. DOA estimation

3.1. DOA estimation of the independent signals

When $K + N_u < M$, the singular value decomposition (SVD) of $\mathbf{C}_x$ is given by

$$\mathbf{C}_x = \mathbf{U}\boldsymbol{\Sigma}\mathbf{V}^H \tag{5}$$

where $\boldsymbol{\Sigma} = \mathrm{diag}\{\lambda_1, \lambda_2, \ldots, \lambda_M\}$ consists of M singular values satisfying $\lambda_1 \geq \cdots \geq \lambda_{K+N_u} > \lambda_{K+N_u+1} = \cdots = \lambda_M = 0$ and $\mathbf{V} \in \mathbb{C}^{M\times M}$ consists of right singular vectors. The columns of $\mathbf{U}_s \triangleq \mathbf{U}(:, 1{:}\ K+N_u)$ are the left singular vectors corresponding to the $K + N_u$ largest singular values, while the columns of $\mathbf{U}_n \triangleq \mathbf{U}(:, K+N_u+1{:}\ M)$ are the left singular vectors corresponding to the $M - K - N_u$ singular values which are all zero. The signal subspace is spanned by the columns of $\mathbf{U}_s$, while the noise subspace is spanned by the columns of $\mathbf{U}_n$. Because the signal subspace is orthogonal to the noise subspace, we have

$$\left\| (\mathbf{A}_{c,k}\boldsymbol{\alpha}_k)^H \mathbf{U}_n \right\|_F^2 = 0, \quad \text{for } k = 1, 2, \ldots, K \tag{6}$$

$$\|\mathbf{a}^H(\theta)\mathbf{U}_n\|_F^2 = 0, \quad \text{for } \theta = \theta_i, \, i = N_c + 1, N_c + 2, \ldots, N. \tag{7}$$

Now denote $z = e^{j\frac{2\pi d}{\lambda}\sin\theta}$, then $\mathbf{a}(z) = [1, z, \ldots, z^{M-1}]^T$. Referring to [15] a root-MUSIC polynomial can be constructed as

$$f(z) \triangleq \mathbf{a}^T(z^{-1})\mathbf{U}_n\mathbf{U}_n^H\mathbf{a}(z). \tag{8}$$

Since $\mathbf{A}_{c,k}$ is a Vandermonde matrix, no linear combination of steering vectors can result in another steering vector, which implies that $f(z)$ will not go to 0 for any coherent signal DOA. Therefore, combined with (7), the roots of (8) $\{z_i\}_{i=1}^{N_u}$ which are closest to the unit circle indicate the desired DOAs of independent sources. The DOA estimates related to the signal roots can be determined as

$$\theta_i = \arcsin\left[\frac{\lambda}{2\pi d}\arg(z_i)\right]. \tag{9}$$

Since $K + N_u$ singular values are much larger than the remaining ones, one can detect $K + N_u$ far-field sources using the popular source enumeration methods [16,17]. However, we will obtain the K roots associated with the K groups of the coherent signals in addition to the roots of the N_u independent signals, which means we have K false DOA estimates. If the number of independent signals is known in advance, then the DOA estimates with the N_u smallest values of $\eta_i = \left\|\mathbf{a}^H(\hat{\theta}_i)\mathbf{U}_n\right\|_F^2$, $i = 1, 2, \ldots, K + N_u$, correspond to the independent signals. However, in practice, the number of independent signals may not be known a priori. As a consequence, it is necessary to provide a more robust criterion to identify the DOA of independent signals from the false ones. Here, we carry out independent signal enumeration inspired by second order statistic of eigenvalues (SORTE) which is a cluster enumeration strategy [18]. Suppose the values of η_i are sorted decreasingly:

$$\eta_1 \ge \eta_2 \ge \cdots \ge \eta_K > \eta_{K+1} = \cdots = \eta_{K+N_u}. \tag{10}$$

To detect the number of independent signals, we define a gap measure:

$$\mathrm{SORTE}(k) = \begin{cases} \dfrac{\mathrm{var}\left(\{\nabla\eta_i\}_{i=k+1}^{K+N_u-1}\right)}{\mathrm{var}\left(\{\nabla\eta_i\}_{i=k}^{K+N_u-1}\right)}, & \mathrm{var}\left(\{\nabla\eta_i\}_{i=k}^{K+N_u-1}\right) \neq 0 \\ +\infty, & \mathrm{var}\left(\{\nabla\eta_i\}_{i=k}^{K+N_u-1}\right) = 0 \end{cases} \tag{11}$$

where $k = 1, 2, \ldots, K + N_u - 2$, $\nabla\eta_i = \eta_i - \eta_{i+1}$, and $\mathrm{var}\left(\{\nabla\eta_i\}_{i=k}^{K+N_u-1}\right) = \frac{1}{K+N_u-k}\sum_{i=k}^{K+N_u-1}\left(\nabla\eta_i - \frac{1}{K+N_u-k}\sum_{l=k}^{K+N_u-1}\nabla\eta_l\right)^2$. Then the number of independent signal is $\hat{N}_u = K + N_u - \arg\min_k \mathrm{SORTE}(k)$.

Remark 1. It can be seen that the proposed method utilises root-MUSIC to classify coherency. Unlike our approach, the authors in [13] partition the whole array into three overlapping subarrays, use ESPRIT to obtain $N_u + K$ DOA estimates, then use a pair matching method to sift the DOA estimates of independent sources. Since that scheme requires an extra subarray, there is a loss of one DOF and reduced array aperture, resulting in a larger DOA estimation error and resolution compared to our technique, especially at low SNRs or limited snapshots. Additionally, since the source enumeration method presented above can distinguish the number of independent signals from the coherent ones, it is applicable to the case without such a priori information which FSDS is not valid for.

3.2. DOA estimation of the coherent signals

Next we will deal with the coherent signals. The coherent signal DOAs are estimated by first removing the independent signals from the FOC matrix $\mathbf{C}_x$ and then the coherent signals are resolved using a novel matrix reconstruction technique for rank restoration. In this way, the proposed method classifies the signal types and provides improved estimation accuracy. The first step in removing the independent signals is estimating their contributions, $\{\bar{\gamma}_i\}_{i=1}^{N_u}$, to the cumulant matrix.

With (5) and (9), we have

$$\bar{\gamma}_i = \frac{1}{\mathbf{a}^H(\theta_i)\mathbf{C}_x^{\ddagger}\mathbf{a}(\theta_i)}, \quad i = 1, 2, \ldots, N_u. \tag{12}$$

The proof of (12) is provided in Appendix A.

From (12), we define $\mathbf{C}_{su} \triangleq \mathrm{diag}\{\bar{\gamma}_1, \ldots, \bar{\gamma}_{N_u}\}$. Given $\mathbf{A}_u$ and $\mathbf{C}_{su}$, we can form a matrix $\mathbf{C}_{xc}$ as

$$\mathbf{C}_{xc} \triangleq \mathbf{C}_x - \mathbf{A}_u\mathbf{C}_{su}\mathbf{A}_u^H = \mathbf{A}_c\boldsymbol{\Gamma}\,\mathrm{diag}\{\bar{\gamma}_{N_u+1}, \ldots, \bar{\gamma}_{N_u+K}\}(\mathbf{A}_c\boldsymbol{\Gamma})^H = \mathbf{A}_c\boldsymbol{\Gamma}\mathbf{C}_{sc}(\mathbf{A}_c\boldsymbol{\Gamma})^H. \tag{13}$$

Clearly, $\mathbf{C}_{xc}$ only contains the information of coherent signals. Note that the FOC of coloured noise will not go to zero in practice due to a limited number of snapshots, which means that the impact of noise can be mitigated but not completely removed, so it is not negligible. For this reason, the smallest singular values $\lambda_{K+N_u+1}, \lambda_{K+N_u+2}, \ldots, \lambda_M$ in (5) are not identical to zero, and their contribution to cumulants can be calculated as $\mathbf{C}_{pn} = \mathbf{U}_n\boldsymbol{\Sigma}_n\mathbf{V}_n^H$ where $\boldsymbol{\Sigma}_n = \mathrm{diag}\{\lambda_{K+N_u+1}, \lambda_{K+N_u+2}, \ldots, \lambda_M\}$ and $\mathrm{V}_n = \mathrm{V}(:, K + N_u + 1: M)$. To alleviate the effect of noise on $\mathbf{C}_{xc}$, the matrix $\mathbf{C}_x$ in (12) and (13) is rectified as $\mathbf{C}_x - \mathbf{C}_{pn}$.

Remark 2. FSDS has implemented this step of eliminating the independent signal contribution from $\mathbf{C}_x$ using spatial differencing. However, part of the coherent signal information (i.e., the entries along the cross diagonal of $\mathbf{C}_x$) will be canceled out in this process as well. As a result, the performance of the subsequent DOA estimation of coherent signals suffers. In contrast, our proposed method achieves the same goal through subtraction of the reconstructed cumulant matrix of independent sources from $\mathbf{C}_x$ without removing any coherent signal information.

After removing the independent source components from $\mathbf{C}_x$, the rank of the remaining coherent signals in $\mathbf{C}_{xc}$ is restored using a matrix reconstruction method.

Here we define a vector $\mathbf{g}_{i,r}$ as

$$\mathbf{g}_{i,r} \triangleq \begin{bmatrix} \mathbf{C}_{xc}(i, m + r - 1) \\ \mathbf{C}_{xc}(i, m + r - 2) \\ \vdots \\ \mathbf{C}_{xc}(i, r) \end{bmatrix}, \quad r = 1, 2, \ldots, L \tag{14}$$

where $L = M + 1 - m$, and construct a matrix $\mathbf{G}_{i,r} = \mathbf{g}_{i,r}\mathbf{g}_{i,r}^H$ accordingly.

Then a new matrix from the i-th row of $\mathbf{C}_{xc}$ is constructed as

$$\bar{\mathbf{C}}_i = \frac{1}{L}\sum_{r=1}^{L}\left(\mathbf{G}_{i,r} + \mathbf{J}\mathbf{G}_{i,r}^{*}\mathbf{J}\right) = \mathbf{B}_c\mathbf{D}_i\mathbf{B}_c^H \tag{15}$$

where

$$\mathbf{B}_c = \mathbf{F}\left[\mathbf{A}_{c,1}, \mathbf{A}_{c,2}, \ldots, \mathbf{A}_{c,K}\right] \tag{16}$$

$$\mathbf{F} = \left[\mathbf{I}_{(M-L+1)}, \mathbf{0}_{(M-L+1)\times(L-1)}\right] \tag{17}$$

$$\mathbf{D}_i = \frac{1}{L}\sum_{r=1}^{L}\left(\boldsymbol{\Phi}^{1-r}\mathbf{d}_i\mathbf{d}_i^H\boldsymbol{\Phi}^{r-1} + \boldsymbol{\Phi}^{r-m}\mathbf{d}_i^{*}\mathbf{d}_i^T\boldsymbol{\Phi}^{m-r}\right) \tag{18}$$

$$\mathbf{\Phi} = \operatorname{diag}\left\{ e^{j\frac{2\pi d}{\lambda}\sin\theta_1}, e^{j\frac{2\pi d}{\lambda}\sin\theta_2}, \ldots, e^{j\frac{2\pi d}{\lambda}\sin\theta_{N_c}} \right\} \tag{19}$$

$$\mathbf{d}_i = \left[d_{11}^{(i)}, \ldots, d_{1P_1}^{(i)}, \ldots, d_{K1}^{(i)}, \ldots, d_{KP_K}^{(i)} \right]^T \tag{20}$$

with

$$d_{kp}^{(i)} = \frac{1}{M}\gamma_k \alpha_{kp}^* e^{-j\frac{2\pi(m-1)d}{\lambda}\sin\theta_{kp}} \sum_{q=1}^{M}\sum_{l=1}^{P_k} \alpha_{kl} e^{j\frac{2\pi(q-1)d}{\lambda}\sin\theta_{kl}} \times \sum_{u=1}^{P_k} \alpha_{ku}^* e^{-j\frac{2\pi(q-1)d}{\lambda}\sin\theta_{ku}} \sum_{v=1}^{P_k} \alpha_{kv} e^{j\frac{2\pi(i-1)d}{\lambda}\sin\theta_{kv}} \tag{21}$$

and $\mathbf{J} \in \mathbb{R}^{m\times m}$ denotes an exchange matrix that has unity entries on the cross diagonal and zeros elsewhere. The proof of (15) can be found in Appendix B.

To further restore the rank and smooth out the effects of noise and limited snapshots, the information of all M rows of $\mathbf{C}_{xc}$ are then utilised to construct an overall smoothed matrix $\bar{\mathbf{C}}$ which is given by

$$\bar{\mathbf{C}} = \sum_{i=1}^{M} \mathbf{B}_c \mathbf{D}_i \mathbf{B}_c^H. \tag{22}$$

Next we examine whether the rank of $\bar{\mathbf{C}}$ has been restored sufficiently to resolve N_c coherent signals.

Proposition 1. *When $m \ge N_c + 1$ and $2L \ge P_{max}$, $\operatorname{rank}(\bar{\mathbf{C}}) = N_c$ for K groups of coherent signals, where $P_{max} = \max\{P_1, P_2, \ldots, P_K\}$.*

The proof of Proposition 1 is given in Appendix C.

One can subsequently follow similar procedures as discussed in Section 3.1 to resolve the DOA estimates of the coherent signals. Particularly, note that $\mathbf{J}\bar{\mathbf{C}}^*\mathbf{J} = \bar{\mathbf{C}}$, which means that $\bar{\mathbf{C}}$ is centro-Hermitian, thus one can transform $\bar{\mathbf{C}}$ into the field of real numbers for the sake of computational efficiency. We define a new matrix $\mathbf{C}_T$ as

$$\mathbf{C}_T = \mathbf{Q}_m^H \bar{\mathbf{C}} \mathbf{Q}_m \tag{23}$$

where $\mathbf{Q}_m$ is a sparse unitary matrix given by

$$\mathbf{Q}_m = \begin{cases} \frac{1}{\sqrt{2}}\begin{bmatrix} \mathbf{I}_n & j\mathbf{I}_n \\ \mathbf{J}_n & -j\mathbf{J}_n \end{bmatrix}, & m = 2n \\ \frac{1}{\sqrt{2}}\begin{bmatrix} \mathbf{I}_n & \mathbf{0}_{n\times1} & j\mathbf{I}_n \\ \mathbf{0}_{n\times1}^T & \sqrt{2} & \mathbf{0}_{n\times1}^T \\ \mathbf{J}_n & \mathbf{0}_{n\times1} & -j\mathbf{J}_n \end{bmatrix}, & m = 2n+1 \end{cases} \tag{24}$$

Referring to Theorem 3 in [19], we can see that $\mathbf{C}_T$ is a real matrix. Then the unitary root-MUSIC polynomial can be expressed as

$$f_U(z) \triangleq \tilde{\mathbf{b}}^T(z^{-1})\mathbf{U}_{Tn}\mathbf{U}_{Tn}^H\tilde{\mathbf{b}}(z) \tag{25}$$

where $\tilde{\mathbf{b}}(z) = \mathbf{Q}_m^H\mathbf{b}(z)$ with $\mathbf{b}(z) = [1, z, \ldots, z^{m-1}]^T$, and the columns of $\mathbf{U}_{Tn}$ are the left singular vectors corresponding to the $m - N_c$ smallest singular values of $\mathbf{C}_T$. The DOA estimates of coherent signals related to the roots $\{z_i\}_{i=1}^{N_c}$ of (25) can be determined by (8) accordingly.

Remark 3. The standard FBSS always exploits the partial information of all rows of $\mathbf{C}_{xc}$ by averaging the cumulants of the subarrays, e.g. submatrices along the main diagonal of $\mathbf{C}_{xc}$, but not utilising the cross correlations between the subarrays, e.g. upper and lower triangular parts of $\mathbf{C}_{xc}$, to resolve the coherent signals, and thus the estimation performance will be compromised to some extent [20]. In contrast, our method exploits all entries of the cumulants matrix of the coherent signals for rank restoration, which means more information has been utilised and better accuracy can be expected.

3.3. Separable signal number

This section discusses the maximum number of separable signals by the proposed scheme. The independent and coherent signals are resolved separately, which makes best use of the DOF of the original ULA and allows more signals than sensors ($N \ge M$) to be estimated, i.e., the so-called underdetermined DOA estimation problem [21,22]. Compared with the standard FBSS which estimates the independent and coherent signals simultaneously, the maximum number of signals estimated by our method can be increased beyond the traditional limit. If $M > K + N_u$, $m > N_c$, and $2L \ge P_{max}$, we can estimate a maximum number of $M - K - 1$ independent sources plus $M - \left\lceil \frac{P_{max}}{2} \right\rceil$ coherent signals since $M \ge N_c + \left\lceil \frac{P_{max}}{2} \right\rceil$, while the FBSS can estimate at most $M - \left\lceil \frac{P_{max}}{2} \right\rceil$ mixed signals since $M \ge N_u + N_c + \left\lceil \frac{P_{max}}{2} \right\rceil$. Although FSDS can also process more signals than array sensors, it has shortcomings in both processing stages. First, FSDS can only handle up to $M - K - 2$ independent signals which is one less than the proposed method as discussed in Remark 1. Besides, FSDS can achieve the same identifiability of coherent signal estimation as our method, but will give rise to a loss of information as explained in Remark 2. Chen et al. [23] used a Toeplitz matrix constructed from the cumulant matrix, referred to as CTMR, to improve the accuracy of DOA estimates no matter whether the sources are coherent or not, but at the cost of halving the DOF and effective array aperture. In general, CTMR's loss of DOF outweighs the gain in accuracy. By exploiting a quite different approach, VESPA in [11,12] achieves much better discrimination of coherent groups, which gives more DOF for estimation with an upper limit of $M - K - 1$ independent sources plus $K\left\lfloor \frac{2M}{3} \right\rfloor$ coherent signals.

Table 1 lists the minimum number of array elements required to resolve a given number of signals by the five methods. For simplicity, we assume that each group has the same number of coherent signals. We can see that our method can use less array elements than most algorithms except VESPA, to estimate the same number of signals.

4. Simulation results and discussion

In this section, a series of numerical experiments under different conditions are conducted to examine the performance of the proposed method. Simulations are carried out for a ULA with half-wavelength spacing between adjacent elements. For simplicity, we assume that all signals, independent and coherent, have identical power. Similar to the settings in [13], the signals are modeled as $\mathbf{s}(t) = \mathbf{F}(t)\mathbf{r}(t)$, where $\mathbf{F}(t) = \operatorname{diag}\{f_1(t), \ldots, f_N(t)\}$, $\mathbf{r}(t) = [r_1(t), \ldots, r_N(t)]^T$. $f_i(t)$ and $r_i(t)$ are zero-mean Gaussian processes with unit-variance and $\sigma_s{}^2$-variance, respectively. The noise is assumed to be a first order spatial autoregressive process, and the (m,n)-th entry of the noise covariance matrix is given by $\mathbf{R}(m, n) = \sigma_n^2 0.8^{|m-n|} e^{j\frac{\pi(m-n)}{16}}$ [24,25]. In order to describe the performance of the source enumeration method we developed in Section 3.1, the detection accuracy is defined as

$$\text{Detection accuracy} = \frac{F_d}{F} \tag{26}$$

where F is the number of trials, and F_d is the number of times that the number of independent signals N_u is successfully detected. The accuracy of the DOA estimate is measured from 800 Monte Carlo

Table 1
Minimum number of array elements required.

Independent signals	Coherent signals		Total signals	Number of array elements				
	Groups	Signals in each group		CTMR	FBSS	FSDS	VESPA	PROPOSED
2	1	2	4	9	5	5	4	4
2	2	2	6	13	7	6	5	5
4	1	4	8	17	10	7	6	6
4	2	2	8	17	9	8	7	7
5	3	2	11	23	12	10	9	9
3	3	3	12	25	14	11	7	11
7	2	4	15	31	17	11	10	10
3	4	4	19	39	21	18	8	18

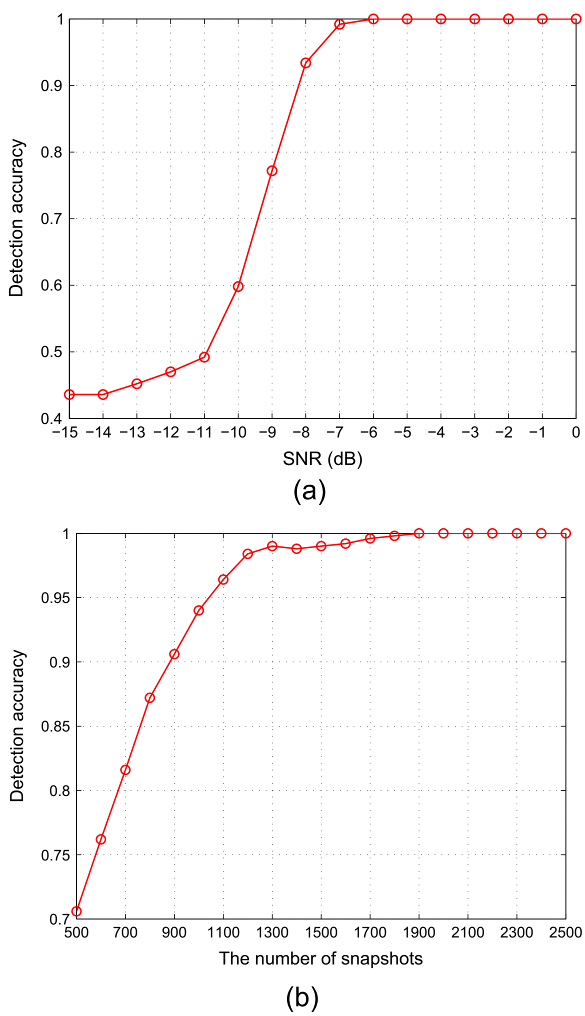

Fig. 1. Detection accuracy versus (a) SNR when the number of snapshots is 2000; (b) the number of snapshots when SNR = − 6 dB.

runs in terms of the root mean square error (RMSE) which is defined as

$$\text{RMSE} = \sqrt{\frac{1}{800N}\sum_{n=1}^{800}\sum_{i=1}^{N}(\hat{\theta}_i^{(n)} - \theta_i)^2} \tag{27}$$

where $\hat{\theta}_i^{(n)}$ is the estimate of θ_i for the n-th trial, and N is the number of all independent or coherent signals. Additionally, to assess the overall reliability of all the algorithms, the probability of resolution is defined as

$$\text{Probability of resolution} = \frac{F_r}{F} \tag{28}$$

where F_r is the number of successful estimations for which the absolute DOA estimation errors of both independent and coherent signals are within 1.5°.

4.1. Source enumeration

In the first scenario, we consider three independent sources from $[-52°, -25°, 27°]$ and two groups of five coherent signals from $[-13°, 37°]$ and $[-39°, 1°, 10°]$, respectively, impinging on an eleven-element array. The fading amplitudes of the coherent signals are $[1, 0.8]$ and $[1, 0.7, 0.6]$, while the fading phases are $[122.16°, 30.52°]$ and $[326.45°, 211.82°, 336.19°]$, respectively. In this case, suppose that this number of independent signals is unknown and we need to detect it. The detection accuracy of the proposed method using as a function of SNR or the number of snapshots is plotted in Fig. 1. Since both FSDS and VESPA do not provide explicit source enumeration methods, there are no counterparts for comparison. We can see that the detection accuracy of our method improves dramatically with increasing SNR or number of snapshots, and achieves a 100% successful detection above −6 dB or 1900 snapshots, which means the enumeration method we developed can even work well under adverse conditions (e.g. relatively low SNRs or few snapshots) for the cumulants.

4.2. DOA estimation

4.2.1. Overdetermined DOA estimation

Since RMSE defined before can only be collected when the number of signals, both independent and coherent, is given, we assume such information is known in advance, or the number of independent signals has been detected successfully using the proposed enumeration approach, and then the number of coherent signals is obtained by the method in [26]. We consider the same scenario as in the source enumeration simulation and select $m=9$ for the reconstruction of $\bar{\mathbf{C}}$. FSDS and VESPA are chosen for comparison. Fig. 2(a) depicts the RMSE of the DOA estimates versus input SNR. The number of snapshots is fixed to 4000. From this figure, we can see that the proposed algorithm has the lowest RMSE for both independent and coherent signals, among all the algorithms for all SNRs. With an increase in SNR, the estimation accuracy of all three algorithms improves, and the RMSE of the independent signals is better than that of coherent signals except for VESPA. Although VESPA can separate coherent groups and achieve more DOF for coherent signal estimation, its performance is not satisfactory due to the large errors introduced by using the

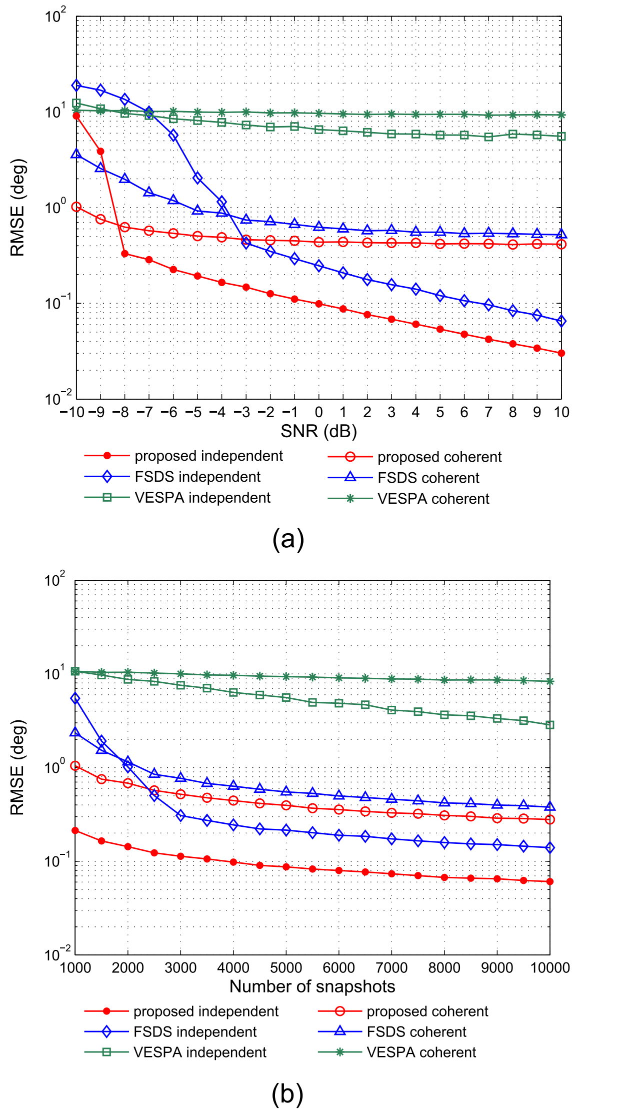

Fig. 2. RMSE of the DOA estimates in the overdetermined case versus (a) SNR when the number of snapshots is 4000; (b) the number of snapshots when SNR = 0 dB.

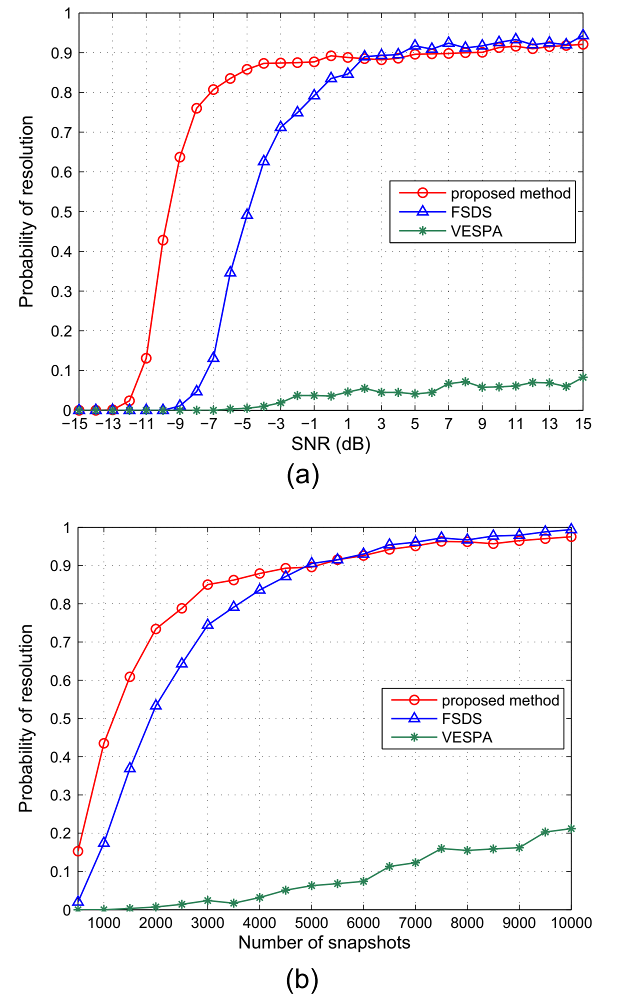

Fig. 3. Probability of resolution of the DOA estimates in the overdetermined case versus (a) SNR when the number of snapshots is 4000; (b) the number of snapshots when SNR = 0 dB.

rotational invariance property to estimate the generalised steering vector. In Fig. 2(b) we show the RMSE performance of all three methods when the number of snapshots increases, fixing the SNR at 0 dB. It is observed that our technique is still superior to FSDS and VESPA, especially when the number of snapshots is less than 3000 for the independent signal case, whereas the performance of FSDS for coherent signal estimation approaches that of the proposed algorithm asymptotically with increasing snapshots. The remaining algorithm, VESPA, however, improves slowly with increasing snapshots and has a relatively large bias for both independent and coherent signals compared with our technique and FSDS even for a relatively large number of samples.

The results of the empirical probability of resolution versus input SNR and the number of snapshots are shown in Fig. 3. It can be observed that the proposed method and FSDS attain over 90% successful estimation above 5 dB. As the SNR decreases, the probability of successful estimation starts dropping for each method at a certain point, known as the SNR threshold, until it eventually becomes zero. The proposed method has the lowest SNR threshold, followed by FSDS and then VESPA which has the highest SNR threshold. Even if the SNR rises to 15 dB, VESPA can barely reach 10% success probability due to the big error in independent signal identification. When the SNR is fixed at 0 dB, both our approach and FSDS can achieve over 90% probability above 5000 snapshots, whereas VESPA can barely reach 20% success probability even if the number of snapshots is greater than 10 000. The proposed method outperforms FSDS, especially at low SNRs or few snapshots, but is somewhat inferior to FSDS when the SNR or the size of snapshots is large.

4.2.2. *Underdetermined DOA estimation*

We consider six independent signals from $[-45°, -26°, -8°, 9°, 24°, 50°]$ and one group of five coherent signals from $[-53°, -33°, -1°, 15°, 41°]$ impinging on a ten-element array. The fading amplitudes and phases of the coherent signals are $[1, 0.7, 0.8, 0.9, 0.6]$ and $[245.97°, 201.89°, 47.96°, 122.01°, 294.69°]$, respectively. We select $m=7$ in this scenario where the total number of signals exceeds the number of array elements.

Fig. 4 depicts the RMSE of DOA estimates in the underdetermined case. From this figure, we can see that as the SNR and the number of snapshots increase, the RMSE of DOA estimation decreases gradually for all of the methods. The proposed method is significantly superior to FSDS and VESPA, especially at low SNRs and few snapshots, mainly because the independent and coherent signals are processed separately while avoiding the elimination of partial coherent information. Although FSDS outperforms VESPA, there is a larger discrepancy between these two and the proposed method even for SNRs up to 10 dB as shown in Fig. 4(a), compared with the first scenario.

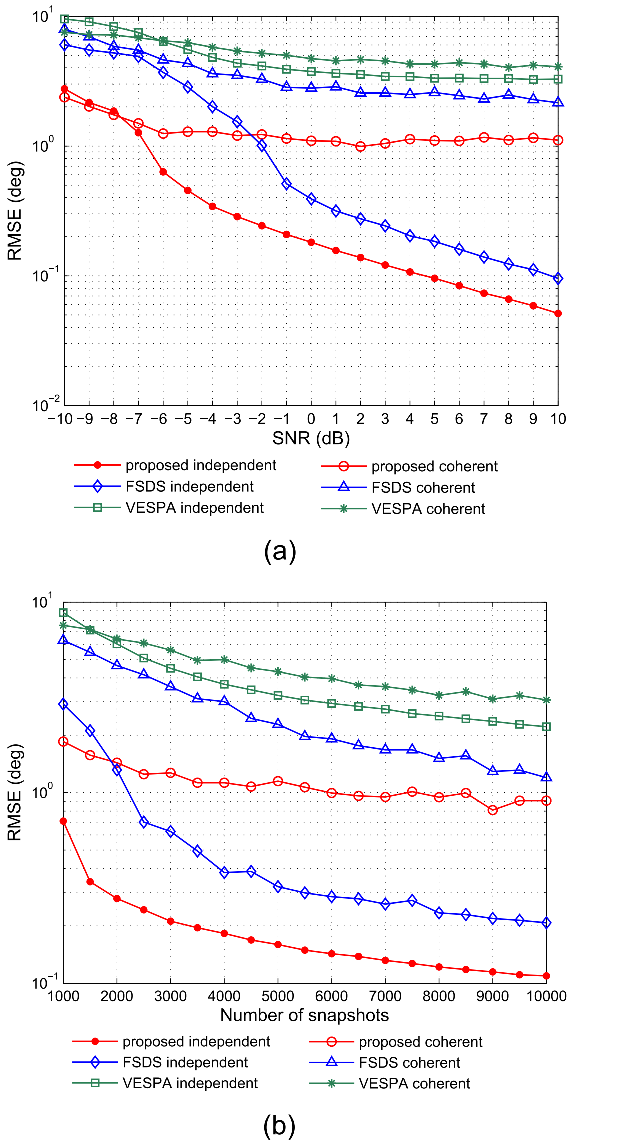

Fig. 4. RMSE of the DOA estimates in the underdetermined case versus (a) SNR when the number of snapshots is 4000; (b) the number of snapshots when SNR = 0 dB.

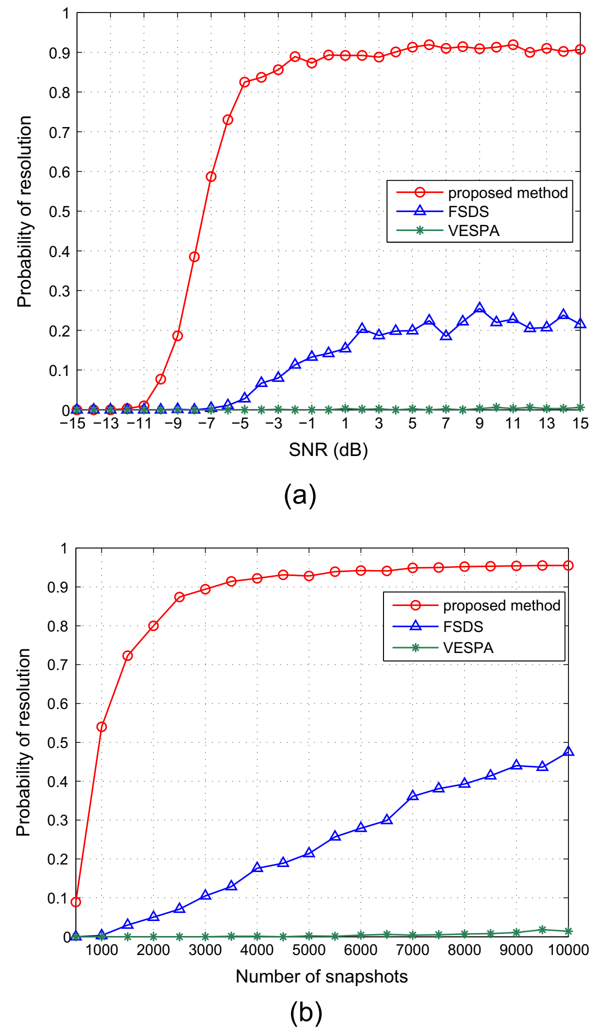

Fig. 5. Probability of resolution of the DOA estimates in the underdetermined case versus (a) SNR when the number of snapshots is 4000; (b) the number of snapshots when SNR = 0 dB.

Next, in Fig. 5 we plot the probability of resolution of the three methods by varying the SNR and total number of snapshots. Evidently the proposed method is superior to the counterparts for all SNRs and number of snapshots considered. Although FSDS outperforms VESPA, both have poor reliability, and there is a clear discrepancy between these two and the proposed method even for snapshot sizes up to 10 000 or beyond 0 dB as shown in the figure.

4.2.3. *Effect of the number of cumulant matrices*

Finally, we test the algorithm in the cases of different numbers of cumulant matrices, denoted as T_m. Consider an independent signal from $-30°$ and one group of three coherent signals from $[-12°, 10°, 33°]$ impinging on a six-element array. The fading amplitudes and phases of the coherent signals are $[1, 0.8, 0.4]$ and $[218.43°, 106.64°, 47.96°]$, respectively. To compare with FSDS, we select $T_m = 1, 6$ for the proposed algorithm. Fig. 6 shows the RMSEs for different values of T_m with respect to SNR and snapshot size, respectively. It can be found that the proposed method is superior to FSDS even though the performance improvement with $T_m = 1$ is not as significant as with $T_m = 6$. It is also worth mentioning that exploiting more cumulant matrices has a clear advantage on coherent signal estimation, compared with independent signal estimation.

5. Conclusion

An FOC-based two-stage matrix reconstruction algorithm is proposed for DOA estimation of mixed independent and coherent signals. The algorithm makes efficient use of the cumulants of sensor outputs of a ULA, and enables us to deal separately with two different types of signals, thus resolving more signals than the number of array elements. At the first stage, the root-MUSIC polynomial is only a function of the DOA of the independent sources while the coherent signals are ignored. At the second stage, the independent components are removed from the cumulant matrix of the received data based on the DOA estimates of the independent sources. Then a matrix reconstruction is performed to restore the rank deficiency in the cumulant matrix of the coherent signals, and finally their DOAs are resolved using a unitary transformation to reduce computation complexity. Compared with previous FOC-based methods, the proposed solution is efficient in the sense that it achieves a more reasonable classification of the signal types, alleviates the array DOF and aperture loss, as well as improves the estimation accuracy of both independent and coherent signals.

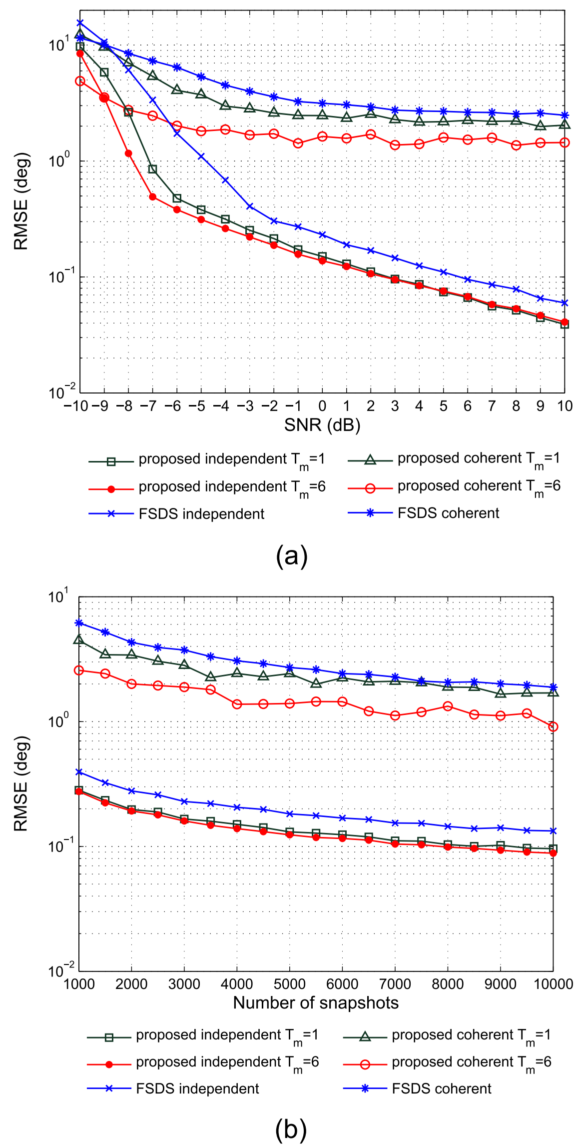

Fig. 6. RMSE of the DOA estimates for T_m versus (a) SNR when the number of snapshots is 4000; (b) the number of snapshots when SNR = 0 dB.

Appendix A. Proof of (12)

Performing the compact SVD of $\bar{\mathbf{A}}$, we have

$$\bar{\mathbf{A}} = \sum_{k=1}^{K+N_u} \eta_k \mathbf{u}_k \mathbf{v}_k^H \tag{A.1}$$

where $\{\eta_k\}_{k=1}^{K+N_u}$, $\{\mathbf{u}_k\}_{k=1}^{K+N_u}$, $\{\mathbf{v}_k\}_{k=1}^{K+N_u}$ are the non-zero singular values, left singular vectors, and right singular vectors, respectively. Accordingly, the pseudo-inverse of $\bar{\mathbf{A}}$ is

$$\bar{\mathbf{A}}^+ = \sum_{k=1}^{K+N_u} \eta_k^{-1} \mathbf{v}_k \mathbf{u}_k^H. \tag{A.2}$$

This allows us to expand the term $\mathbf{a}^H(\theta_i)\mathbf{C}_x^+\mathbf{a}(\theta_i)$ as

$$\begin{aligned}\mathbf{a}^H(\theta_i)\mathbf{C}_x^+\mathbf{a}(\theta_i) &= \mathbf{a}^H(\theta_i)\left(\bar{\mathbf{A}}^H\right)^+\mathbf{C}_s^{-1}\bar{\mathbf{A}}^+\mathbf{a}(\theta_i)\\ &= \left(\bar{\mathbf{A}}^+\mathbf{a}(\theta_i)\right)^H\mathbf{C}_s^{-1}\bar{\mathbf{A}}^+\mathbf{a}(\theta_i).\end{aligned} \tag{A.3}$$

Note that $\bar{\mathbf{A}} = [\mathbf{a}(\theta_i), \mathbf{B}]$, $i = 1, 2, \ldots, N_u$, where $\mathbf{B}$ is the remaining part of $\bar{\mathbf{A}}$, one has $\mathbf{a}(\theta_i) = \bar{\mathbf{A}}\mathbf{e}_i$ where $\mathbf{e}_i \in \mathbb{R}^{K+N_u}$ is a column vector with 1 at the i-th entry and 0 elsewhere, then substitute it back to (A.3),

$$\begin{aligned}\mathbf{a}^H(\theta_i)\mathbf{C}_x^+\mathbf{a}(\theta_i) &= \left(\sum_{k=1}^{K+N_u}\eta_k^{-1}\mathbf{v}_k\mathbf{u}_k^H\sum_{k=1}^{K+N_u}\eta_k\mathbf{u}_k\mathbf{v}_k^H\mathbf{e}_i\right)^H\mathbf{C}_s^{-1}\\ &\quad\times\sum_{k=1}^{K+N_u}\eta_k^{-1}\mathbf{v}_k\mathbf{u}_k^H\sum_{k=1}^{K+N_u}\eta_k\mathbf{u}_k\mathbf{v}_k^H\mathbf{e}_i = \mathbf{e}_i^H\mathbf{C}_s^{-1}\mathbf{e}_i\\ &= \mathbf{e}_i^H\mathrm{diag}\{\bar{\gamma}_1^{-1}, \ldots, \bar{\gamma}_{K+N_u}^{-1}\}\mathbf{e}_i = \bar{\gamma}_i^{-1}.\end{aligned} \tag{A.4}$$

Therefore,

$$\bar{\gamma}_i = \frac{1}{\mathbf{a}^H(\theta_i)\mathbf{C}_x^+\mathbf{a}(\theta_i)}, \quad i = 1, 2, \ldots, N_u \tag{A.5}$$

and this proves (12).

Appendix B. Proof of (15)

Since $\mathbf{C}_{xc}$ only contains the information of coherent signals, from the received data model given in (1) the snapshot of coherent signals at the i-th sensor can be expressed as

$$x_{c,i}(t) = \sum_{k=1}^{K}\sum_{p=1}^{P_k}\alpha_{kp}s_k(t)e^{j\frac{2\pi(i-1)d}{\lambda}\sin\theta_{kp}}. \tag{B.1}$$

By the definition of cumulants we have

$$\begin{aligned}
\mathbf{C}_{xc}(i,m+r-n) &= \frac{1}{M}\sum_{q=1}^{M}\mathrm{cum}\{x_{c,q}(t),x_{c,q}^*(t),x_{c,i}(t),x_{c,m+r-n}^*(t)\}\\
&= \frac{1}{M}\sum_{q=1}^{M}\mathrm{cum}\Bigg\{\sum_{k=1}^{K}\sum_{p=1}^{P_k}\alpha_{kp}s_k(t)e^{j\frac{2\pi(q-1)d}{\lambda}\sin\theta_{kp}},\\
&\quad\sum_{k=1}^{K}\sum_{p=1}^{P_k}\alpha_{kp}^*s_k^*(t)e^{-j\frac{2\pi(q-1)d}{\lambda}\sin\theta_{kp}},\\
&\quad\sum_{k=1}^{K}\sum_{p=1}^{P_k}\alpha_{kp}s_k(t)e^{j\frac{2\pi(i-1)d}{\lambda}\sin\theta_{kp}},\\
&\quad\sum_{k=1}^{K}\sum_{p=1}^{P_k}\alpha_{kp}^*s_k^*(t)e^{-j\frac{2\pi(m+r-n-1)d}{\lambda}\sin\theta_{kp}}\Bigg\}\\
&= \frac{1}{M}\sum_{q=1}^{M}\sum_{k=1}^{K}\sum_{l=1}^{P_k}\alpha_{kl}e^{j\frac{2\pi(q-1)d}{\lambda}\sin\theta_{kl}}\\
&\quad\times\sum_{u=1}^{P_k}\alpha_{ku}^*e^{-j\frac{2\pi(q-1)d}{\lambda}\sin\theta_{ku}}\sum_{v=1}^{P_k}\alpha_{kv}e^{j\frac{2\pi(i-1)d}{\lambda}\sin\theta_{kv}}\\
&\quad\times\sum_{p=1}^{P_k}\alpha_{kp}^*e^{-j\frac{2\pi(m+r-n-1)d}{\lambda}\sin\theta_{kp}}\mathrm{cum}\{s_k(t),s_k^*(t),s_k(t),s_k^*(t)\}\\
&= \sum_{k=1}^{K}\sum_{p=1}^{P_k}\frac{1}{M}\gamma_k\alpha_{kp}^*e^{-j\frac{2\pi(m+r-n-1)d}{\lambda}\sin\theta_{kp}}\\
&\quad\times\sum_{q=1}^{M}\sum_{l=1}^{P_k}\alpha_{kl}e^{j\frac{2\pi(q-1)d}{\lambda}\sin\theta_{kl}}\sum_{u=1}^{P_k}\alpha_{ku}^*e^{-j\frac{2\pi(q-1)d}{\lambda}\sin\theta_{ku}}\\
&\quad\times\sum_{v=1}^{P_k}\alpha_{kv}e^{j\frac{2\pi(i-1)d}{\lambda}\sin\theta_{kv}}.
\end{aligned}\tag{B.2}$$

If we define $a_{kp}\triangleq e^{j\frac{2\pi(n-1)d}{\lambda}\sin\theta_{kp}}$, $\mathbf{d}_i\triangleq\left[d_{11}^{(i)},\dots,d_{1P_1}^{(i)},\dots,d_{K1}^{(i)},\dots,d_{KP_K}^{(i)}\right]^T$ with

$$\begin{aligned}
d_{kp}^{(i)} &= \frac{1}{M}\gamma_k\alpha_{kp}^*e^{-j\frac{2\pi(m-1)d}{\lambda}\sin\theta_{kp}}\sum_{q=1}^{M}\sum_{l=1}^{P_k}\alpha_{kl}e^{j\frac{2\pi(q-1)d}{\lambda}\sin\theta_{kl}}\\
&\quad\times\sum_{u=1}^{P_k}\alpha_{ku}^*e^{-j\frac{2\pi(q-1)d}{\lambda}\sin\theta_{ku}}\sum_{v=1}^{P_k}\alpha_{kv}e^{j\frac{2\pi(i-1)d}{\lambda}\sin\theta_{kv}}
\end{aligned}\tag{B.3}$$

the above equation can be rewritten in the following compact format:

$$\mathbf{C}_{xc}(i,m+r-n) = \left[a_{11},\dots,a_{1P_1},\dots,a_{K1},\dots,a_{KP_K}\right]\boldsymbol{\Phi}^{1-r}\mathbf{d}_i, \tag{B.4}$$

where $\boldsymbol{\Phi}=\mathrm{diag}\{e^{j\frac{2\pi d}{\lambda}\sin\theta_1},e^{j\frac{2\pi d}{\lambda}\sin\theta_2},\dots,e^{j\frac{2\pi d}{\lambda}\sin\theta_{N_c}}\}$. Stacking $\mathbf{C}_{xc}(i,m+r-1),\mathbf{C}_{xc}(i,m+r-2),\dots,\mathbf{C}_{xc}(i,r)$ in a column, we obtain

$$\mathbf{g}_{i,r} = \mathbf{F}\left[\mathbf{A}_{c,1},\dots,\mathbf{A}_{c,K}\right]\boldsymbol{\Phi}^{1-r}\mathbf{d}_i = \mathbf{B}_c\boldsymbol{\Phi}^{1-r}\mathbf{d}_i,\quad r=1,2,\dots,L \tag{B.5}$$

where $\mathbf{F}=\left[\mathbf{I}_{(M-L+1)},\mathbf{0}_{(M-L+1)\times(L-1)}\right]$, $\mathbf{B}_c=\mathbf{F}\left[\mathbf{A}_{c,1},\dots,\mathbf{A}_{c,K}\right]$, and further $\mathbf{G}_{i,r}=\mathbf{B}_c\boldsymbol{\Phi}^{1-r}\mathbf{d}_i\mathbf{d}_i^H\boldsymbol{\Phi}^{r-1}\mathbf{B}_c^H$.

Since $\mathbf{B}_c$ is a Vandermonde matrix, it can be readily seen that $\mathbf{J}\mathbf{B}_c^*=\mathbf{B}_c\boldsymbol{\Phi}^{1-m}$ where $\mathbf{J}\in\mathbb{R}^{m\times m}$ is an exchange matrix. Then one has

$$\begin{aligned}
\bar{\mathbf{C}}_i &= \frac{1}{L}\sum_{r=1}^{L}\left(\mathbf{G}_{i,r}+\mathbf{J}\mathbf{G}_{i,r}^*\mathbf{J}\right)\\
&= \mathbf{B}_c\left(\frac{1}{L}\sum_{r=1}^{L}\left(\boldsymbol{\Phi}^{1-r}\mathbf{d}_i\mathbf{d}_i^H\boldsymbol{\Phi}^{r-1}+\boldsymbol{\Phi}^{r-m}\mathbf{d}_i^*\mathbf{d}_i^T\boldsymbol{\Phi}^{m-r}\right)\right)\mathbf{B}_c^H\\
&= \mathbf{B}_c\mathbf{D}_i\mathbf{B}_c^H
\end{aligned}\tag{B.6}$$

and this proves (15).

Appendix C. Proof of Proposition 1

Under the assumptions that $\mathbf{A}_c$ is unambiguous and $m\ge N_c+1$, the rank of the Vandermonde matrix $\mathbf{B}_c$ is given by $\mathrm{rank}(\mathbf{B}_c)=N_c$. Since $\mathbf{D}_i$ can be rewritten as

$$\begin{aligned}
\mathbf{D}_i &= \frac{1}{L}\left[\boldsymbol{\Phi}^{1-L}\mathbf{d}_i,\boldsymbol{\Phi}^{2-L}\mathbf{d}_i,\dots,\mathbf{d}_i,\boldsymbol{\Phi}^{1-m}\mathbf{d}_i^*,\boldsymbol{\Phi}^{2-m}\mathbf{d}_i^*,\dots,\boldsymbol{\Phi}^{L-m}\mathbf{d}_i^*\right]\\
&\quad\times\left[\boldsymbol{\Phi}^{1-L}\mathbf{d}_i,\boldsymbol{\Phi}^{2-L}\mathbf{d}_i,\dots,\mathbf{d}_i,\boldsymbol{\Phi}^{1-m}\mathbf{d}_i^*,\boldsymbol{\Phi}^{2-m}\mathbf{d}_i^*,\dots,\boldsymbol{\Phi}^{L-m}\mathbf{d}_i^*\right]^H\\
&= \frac{1}{L}\mathbf{T}_i\left[\mathbf{V},\mathbf{HV}\right]\left[\mathbf{V},\mathbf{HV}\right]^H\mathbf{T}_i^H
\end{aligned}\tag{C.1}$$

where

$$\begin{aligned}
\mathbf{T}_i = \mathrm{diag}\Bigg\{&e^{j\frac{2\pi(1-L)d}{\lambda}\sin\theta_{11}}d_{11}^{(i)},\dots,e^{j\frac{2\pi(1-L)d}{\lambda}\sin\theta_{1P_1}}d_{1P_1}^{(i)},\dots,\\
&e^{j\frac{2\pi(1-L)d}{\lambda}\sin\theta_{K1}}d_{K1}^{(i)},\dots,e^{j\frac{2\pi(1-L)d}{\lambda}\sin\theta_{KP_K}}d_{KP_K}^{(i)}\Bigg\},
\end{aligned}$$

$\mathbf{V}=\mathbf{A}_c^T(1:L,1:N_c)$, and

$$\begin{aligned}
\mathbf{H} = \mathrm{diag}\Bigg\{&\frac{d_{11}^{*(i)}}{d_{11}^{(i)}}e^{j\frac{2\pi(1-m)d}{\lambda}\sin\theta_{11}},\dots,\frac{d_{1P_1}^{*(i)}}{d_{1P_1}^{(i)}}e^{j\frac{2\pi(1-m)d}{\lambda}\sin\theta_{1P_1}},\dots,\\
&\frac{d_{K1}^{*(i)}}{d_{K1}^{(i)}}e^{j\frac{2\pi(1-m)d}{\lambda}\sin\theta_{K1}},\dots,\frac{d_{KP_K}^{*(i)}}{d_{KP_K}^{(i)}}e^{j\frac{2\pi(1-m)d}{\lambda}\sin\theta_{KP_K}}\Bigg\}\\
\triangleq{}&\mathrm{diag}\{h_1,h_2,\dots,h_{N_c}\}.
\end{aligned}$$

It is easy to identify that $\mathrm{rank}(\mathbf{T}_i)=\mathrm{rank}(\mathbf{H})=N_c$, $\mathrm{rank}(\mathbf{V})=\min(L,N_c)$. Referring to [5], we know that $\mathrm{rank}(\mathbf{D}_i)=\mathrm{rank}([\mathbf{V},\mathbf{HV}])=\min\{2L,N_c\}\ge P_{max}$ under the mild restriction that whenever equality holds among some of the members of the set $\{h_i\}_{i=1}^{N_c}$, the largest subset with equal entries must at most be of size L.

We know that $\mathbf{C}_{xc}=\mathbf{A}_c\boldsymbol{\Gamma}\mathbf{C}_{sc}(\mathbf{A}_c\boldsymbol{\Gamma})^H$, $\mathrm{rank}(\mathbf{A}_c)=N_c$, $\mathrm{rank}(\boldsymbol{\Gamma})=\mathrm{rank}(\mathbf{C}_{sc})=K$, so $\mathrm{rank}(\mathbf{C}_{xc})=K$. This implies that the size of the largest collection of linearly independent rows of $\mathbf{C}_{xc}$ is K. Without loss of generality, we assume the largest collection of linearly independent rows is $\{\mathbf{C}_{xc}(i,:)\}_{i=1}^{K}$. Since the matrix $[\mathbf{C}_{xc}(1,:),\mathbf{C}_{xc}(2,:),\dots,\mathbf{C}_{xc}(K,:)]=[\mathbf{B}_c\boldsymbol{\Psi}\mathbf{d}_1,\mathbf{B}_c\boldsymbol{\Psi}\mathbf{d}_2,\dots,\mathbf{B}_c\boldsymbol{\Psi}\mathbf{d}_K]=\mathbf{B}_c\boldsymbol{\Psi}[\mathbf{d}_1,\mathbf{d}_2,\dots,\mathbf{d}_K]$ where

$$\boldsymbol{\Psi}=\mathrm{diag}\left\{e^{-j\frac{2\pi(M-m)d}{\lambda}\sin\theta_1},e^{-j\frac{2\pi(M-m)d}{\lambda}\sin\theta_2},\dots,e^{-j\frac{2\pi(M-m)d}{\lambda}\sin\theta_{N_c}}\right\},$$

the vectors $\{\mathbf{d}_i\}_{i=1}^{K}$ are linearly independent to each other, and further matrices $\{\mathbf{T}_i\}_{i=1}^{K}$ are linearly independent to each other as well.

Denote $\mathbf{W}=[\mathbf{V},\mathbf{HV}]$, we have

$$\sum_{i=1}^{K}\mathbf{D}_i=\frac{1}{L}\left[\mathbf{T}_1\mathbf{W},\mathbf{T}_2\mathbf{W},\dots,\mathbf{T}_K\mathbf{W}\right]\left[\mathbf{T}_1\mathbf{W},\mathbf{T}_2\mathbf{W},\dots,\mathbf{T}_K\mathbf{W}\right]^H \tag{C.2}$$

As discussed above, $c_1\mathbf{T}_1+c_2\mathbf{T}_2+\cdots+c_K\mathbf{T}_K=\mathbf{0}$ holds if and only if $c_1=c_2=\cdots=c_K=0$, and thus $(c_1\mathbf{T}_1+c_2\mathbf{T}_2+\cdots+c_K\mathbf{T}_K)\mathbf{W}=c_1\mathbf{T}_1\mathbf{W}+c_2\mathbf{T}_2\mathbf{W}+\cdots+c_K\mathbf{T}_K\mathbf{W}=\mathbf{0}$ under the same condition. This implies that matrices $\{\mathbf{T}_i\mathbf{W}\}_{i=1}^{K}$ are linearly independent to each other. Therefore, $\mathrm{rank}\left(\sum_{i=1}^{K}\mathbf{D}_i\right)=\mathrm{rank}([\mathbf{T}_1\mathbf{W},\mathbf{T}_2\mathbf{W},\dots,\mathbf{T}_K\mathbf{W}])=\min\{2KL,N_c\}=N_c$.

It can be seen that $\{\mathbf{D}_i\}_{i=K+1}^{M}$ do not contribute to the rank recovery as each of the remaining matrices $\{\mathbf{T}_i\mathbf{W}\}_{i=K+1}^{M}$ can be expressed as a linear combination of $\{\mathbf{T}_i\mathbf{W}\}_{i=1}^{K}$, and consequently $\mathrm{rank}(\bar{\mathbf{C}})=\mathrm{rank}\left(\sum_{i=1}^{M}\mathbf{D}_i\right)=N_c$. This completes the proof of Proposition 1.

References

[1] H. Krim, M. Viberg, Two decades of array signal processing research: the parametric approach, IEEE Signal Process. Mag. 13 (4) (1996) 67–94.

[2] R.O. Schmidt, Multiple emitter location and signal parameter estimation, IEEE Trans. Antennas Propag. 34 (3) (1986) 276–280.

[3] R. Roy, T. Kailath, ESPRIT – estimation of signal parameters via rotational invariance techniques, IEEE Trans. Acoust. Speech Signal Process. 37 (7) (1989) 984–995.

[4] T.J. Shan, M. Wax, T. Kailath, On spatial smoothing for direction-of-arrival estimation of coherent signals, IEEE Trans. Acoust. Speech Signal Process. 33 (4) (1985) 806–811.

[5] S.U. Pillai, B.H. Kwon, Forward/backward spatial smoothing techniques for coherent signal identification, IEEE Trans. Acoust. Speech Signal Process. 37 (1) (1989) 8–15.

[6] F.M. Han, X.D. Zhang, An ESPRIT-like algorithm for coherent DOA estimation, IEEE Antennas Wirel. Propag. Lett. 4 (1) (2005) 443–446.

[7] R. Rajagopal, P.R. Rao, Generalized algorithm for DOA estimation in a passive sonar, IEE Proc. F, Radar Signal Process. 140 (1) (1993) 12–20.

[8] C. Qi, Y. Wang, Y. Zhang, Y. Han, Spatial difference smoothing for DOA estimation of coherent signals, IEEE Signal Process. Lett. 12 (11) (2005) 800–802.

[9] Z. Ye, Y. Zhang, X. Xu, C. Liu, Direction of arrival estimation for uncorrelated and coherent signals with uniform linear array, IET Radar Sonar Navig. 3 (4) (2009) 144–154.

[10] Y. Zhang, Z. Ye, Efficient method of DOA estimation for uncorrelated and coherent signals, IEEE Antennas Wirel. Propag. Lett. 7 (2008) 799–802.

[11] E. Gönen, J.M. Mendel, Applications of cumulants to array processing – part III: blind beamforming for coherent signals, IEEE Trans. Signal Process. 45 (9) (1997) 2252–2264.

[12] E. Gönen, J.M. Mendel, M.C. Dǒgan, Applications of cumulants to array processing – part IV: direction finding in coherent signals case, IEEE Trans. Signal Process. 45 (9) (1997) 2265–2276.

[13] Z. Ye, Y. Zhang, DOA estimation for non-Gaussian signals using fourth-order cumulants, IET Microw. Antennas Propag. 3 (7) (2009) 1069–1078.

[14] J.M. Mendel, Tutorial on higher-order statistics (spectra) in signal processing and system theory: theoretical results and some applications, Proc. IEEE 79 (3) (1991) 278–305.

[15] B.D. Rao, K.V.S. Hari, Performance analysis of Root-MUSIC, IEEE Trans. Acoust. Speech Signal Process. 37 (12) (1989) 1939–1949.

[16] M. Wax, T. Kailath, Detection of signals by information theoretic criteria, IEEE Trans. Acoust. Speech Signal Process. 33 (2) (1985) 387–392.

[17] H.-T. Wu, J.-F. Yang, F.-K. Chen, Source number estimators using transformed Gerschgorin radii, IEEE Trans. Signal Process. 43 (6) (1995) 1325–1333.

[18] Z. He, A. Cichocke, S. Xie, K. Choi, Detecting the number of clusters in n-way probabilistic clustering, IEEE Trans. Pattern Anal. Mach. Intell. 32 (11) (2010) 2006–2021.

[19] N. Yilmazer, J. Koh, T.K. Sarkar, Utilization of a unitary transform for efficient computation in the matrix pencil method to find the direction of arrival, IEEE Trans. Antennas Propag. 54 (1) (2006) 175–181.

[20] W. Du, R.L. Kirlin, Improved spatial smoothing techniques for DOA estimation of coherent signals, IEEE Trans. Signal Process. 39 (5) (1991) 1208–1210.

[21] W.-K. Ma, T.-H. Hsieh, C.-Y. Chi, Direction-of-arrival estimation of quasistationary signals with less sensors than sources and unknown spatial noise covariance: a Khatri–Rao subspace approach, IEEE Trans. Signal Process. 58 (4) (2010) 2168–2180.

[22] P. Pal, P.P. Vaidyanathan, Nested arrays: a novel approach to array processing with enhanced degrees of freedom, IEEE Trans. Signal Process. 58 (8) (2010) 4167–4181.

[23] H. Chen, C. Hou, Q. Wang, L. Huang, W. Yan, Cumulants-based Toeplitz matrices reconstruction method for 2-D coherent DOA estimation, IEEE Sens. J. 14 (8) (2014) 2824–2832.

[24] K.M. Wong, J.P. Reilly, Q. Wu, S. Qiao, Estimation of the directions of arrival of signals in unknown correlated noise, part I: the MAP approach and its implementation, IEEE Trans. Signal Process. 40 (8) (1992) 2007–2017.

[25] M. Viberg, P. Stoica, B. Ottersten, Maximum likelihood array processing in spatially correlated noise fields using parameterized signals, IEEE Trans. Signal Process. 45 (4) (1997) 996–1004.

[26] J.H. Cozzens, M.J. Sousa, Source enumeration in a correlated signal environment, IEEE Trans. Signal Process. 42 (2) (1994) 304–317.